Case Studies in Thermal Engineering 51 (2023) 103657

Contents lists available at ScienceDirect

Case Studies in Thermal Engineering

journal homepage: www.elsevier.com/locate/csite

Comparison of the flame stabilities during oxy-methane and air-methane combustion in a two-layer porous burner

Mingjian Liao [a,b], Zhu He [a,b], Shuyuan Jia [a,b], Xiong Liang [a,b], Tat Leung Chan [c,d], Yawei Li [a,b], Xuecheng Xu [b], Ting Liu [a,b,*]

[a] The State Key Laboratory of Refractories and Metallurgy, Wuhan University of Science and Technology, Wuhan, 430081, PR China
[b] National-provincial Joint Engineering Research Center of High Temperature Materials and Lining Technology, Wuhan, 430081, PR China
[c] Department of Mechanical Engineering, The Hong Kong Polytechnic University, Hong Kong SAR, PR China
[d] The Hong Kong Polytechnic University, Shenzhen Research Institute, Shenzhen, PR China

ARTICLE INFO

Handling Editor: Huihe Qiu

Keywords:
Porous media combustion
Oxy-fuel
Flame stabilization

ABSTRACT

The development of the oxy-fuel porous media combustion technique not only takes advantage of the characteristics of porous media combustion, such as a relatively low lean-burn limit and small volume, but also dramatically facilitates carbon capture and storage. In this paper, a two-layer porous burner model is established, in which a two-temperature equation model is adopted for calculation purposes. Differences in combustion behaviour between oxy-fuel and air-fuel conditions are compared. The results show that the difference in physical properties between CO_2 and air is the main reason for the significant variation of combustion behaviours under the conditions of oxy-fuel compared to air-fuel. The specific performance is lower combustion temperature and flame propagation speed. The temperature under oxy-fuel combustion conditions is 300 K lower than that under air-fuel combustion conditions at an equivalence ratio of 0.6, and the stable range of oxy-fuel combustion is only approximately 50% of air-fuel combustion. The impact of porous media material parameters on combustion behavior has been investigated. These variables include the equivalence ratio, material thermal conductivity, volume heat transfer coefficient, and extinction coefficient, while the ratio of O_2/CO_2 remains fixed at 0.21/0.79. The influence of these variables on the stable velocity range and temperature field is consistent, but a large difference in values occurs. Reducing the thermal resistance of the burner by adjusting the properties of the porous matrix can increase the velocity limit of stable combustion. However, even if the thermal conductivity and extinction coefficient are increased by 5 times, there will be no significant impact on the stable range. Reducing the pore size of the combustion zone by 50% will increase the stable range by over 100%.

1. Introduction

Greenhouse gas (GHG) anthropogenic emissions into the atmosphere are the ultimate cause of current climate change [1]. The CO_2 produced by the burning of fossil fuels is the main part of anthropogenic GHG emissions [2]. Among the CO_2 emission reduction techniques, carbon capture and storage (CCS) is considered to be the most economical and feasible way to reduce GHG emissions on a

* Corresponding author. Department of Thermal Energy Engineering School of Materials and Metallurgy Wuhan University of Science and Technology Wuhan 430081, PR China.
E-mail address: liuting666@wust.edu.cn (T. Liu).

https://doi.org/10.1016/j.csite.2023.103657
Received 29 August 2022; Received in revised form 12 October 2023; Accepted 20 October 2023
Available online 20 October 2023

large scale in the future [3]. The oxy-fuel combustion technique is one of the crucial categorizations of CCS In the oxy-fuel combustion process, pure oxygen is employed for fuel combustion, resulting in only H_2O and CO_2 as products. After separation by CCS, the CO_2 is prevented from being directly discharged into the environment, and the actual zero CO_2 emission is realized [4,5]. Moreover, the combustion-supporting gas does not contain N_2, so it does not produce any form of NO_x.

At present, the oxy-fuel combustion technique has been widely applied in various solid-fuel industrial kilns in the fields of metallurgy and thermal energy. It has produced apparent effects in the improvement of furnace efficiency and environmental protection, such as pulverized coal boilers and circulating fluidized beds [6–8]. However, the flame propagation rate of oxy-fuel combustion is low, and local high temperature and uneven temperature fields often exist in the combustion chamber, resulting in its low combustion efficiency [9]. The porous media combustion (PMC) technology will significantly broaden the burn limit of gaseous fuels, which is conducive to improving combustion efficiency and reducing pollutant emissions [10,11]. In the process of porous media combustion, the solid porous matrix significantly affects flame behaviour. The heat generated during the combustion process is recovered by convective heat transfer to the solid matrix. Meanwhile, the recovered heat is continuously transferred upstream via conduction and radiation of the solid matrix, thus resulting in preheating of the unburned gas. As a result, the flame temperature of PMC is usually higher than that of adiabatic combustion. Therefore, the combustion efficiency of fuel is improved, and the lean-burn limit is notably broadened. Meanwhile, as the chemical heat release is transferred fractionally through the solid matrix, the burner's temperature is relatively uniform. The problems of a high temperature and poor temperature uniformity in oxy-fuel combustion are thus suitably addressed [9]. Owing to these specific advantages, oxy-fuel combined with PMC may be a potential clean combustion technique.

However, the flame generated during PMC is difficult to stabilize at a certain position in the burner, which indicates that the position of the flame continuously moves over time. Therefore, many burner structures have been designed to stabilize the flame position. One of the simple and effective designs is the superposition of two porous medium matrixes of different porosities and pore diameters, which could stabilize the flame near the interface under certain working conditions [12–14]. At present, there are many studies on two-layer porous burners. Gao et al. [12] conducted experimental studies on the combustion of methane/air mixtures in a two-layer porous burner. The combustion behaviors under solid matrix with different pore structures were compared. The flame temperature, stability, and pollutant emissions were completely different under the same working conditions. In addition, material properties such as the pore diameter, porosity, and thermal conductivity imposed a significant effect on the temperature field and spread velocity of the flame [15]. In other experiments, operational parameters such as equivalence ratio, fuel composition, and inlet velocity have also been shown to play important roles in flame temperature, radiation intensity, and stability [16,17]. However, some shortcomings in experimental research have also been found. Because thermocouples are generally discretely inserted into the porous medium matrix, the flame position and peak temperature may be difficult to capture [18]. Therefore, numerical methods have also been adopted by many researchers to study the combustion process, hoping to obtain a complete temperature field. Nevertheless, due to the complex pore structure of porous medium materials, primarily ceramic foams, the physical structure is challenging to model geometrically directly [19,20]. Consequently, simplified porous models have been widely applied to solve the temperature field. In early one-temperature equation models, the temperature of the solid porous matrix was regarded as equal to that of the gas field, and the physical properties of the solid matrix were directly added to the temperature equation to solve the problem [21]. Many researchers have recently proposed that the temperature difference between the gas and the solid phase cannot be ignored. Hence, an additional temperature equation has been added to consider the solid matrix separately. This is called the two-temperature equation model. Based on this model, José et al. [22] studied the influence of the inlet velocity, excess air coefficient, porosity, and thermal conductivity of the porous material on the temperature field. It was pointed out that a decrease in the porosity could accelerate the preheating process of the unburned gas and reduce the peak temperature of the flame. Increasing the thermal conductivity of the porous material in the preheating zone could reduce the temperature gradient and flame peak temperature in the burner, but flashback could easily occur. However, increasing the thermal conductivity of the combustion zone exerted little effect on the temperature. Barra et al. [23] investigated the effects of the equivalence ratio, material thermal conductivity, volume heat transfer coefficient, and extinction coefficient on the flame stability. Its conclusions reveal the sensitivity of these variables to flame stability. Shi et al. [24] evaluated the fuel-rich combustion process in a porous matrix and pointed out that the thermal conductivity of the porous medium material yields a great impact on the temperature field. Increasing the thermal conductivity of the material could reduce the peak temperature and greatly affect the production of CO. Our previous study [25] focused on flame stability during premixed oxy-methane combustion in porous media. Based on the CFD solver OpenFOAM (version 8) coupled with OpenSMOKE++, numerical models of a two-layer porous burner are established. Combined with the methane skeletal kinetic mechanism, the laminar combustion process in the porous media burner is simulated. It pointed out the potential drawbacks of oxy-fuel PMC, namely its narrow stable range and high CO emissions. It was revealed that flame temperature is a significant factor influencing the stable range. Increasing the flame temperature (such as increasing equivalence ratio, oxidizer ratio, or preheating the fresh fuel gas) can broaden the stable limit. However, the fundamental causes for the narrow flammability range remain unclear.

Stable combustion is a prerequisite for the promotion and application of PMC technology. Most of the researchers mentioned above have proposed many methods to improve its stability, such as adjusting the physical property parameters of porous matrix or operational parameters. However, most of these studies were conducted under air-fuel conditions. The research on the combination of PMC and oxy-fuel technology is relatively lacking. The physical properties of CO_2 and N_2 are completely different, for example, the density of the former at room temperature is 145% of that of the latter, and its thermal conductivity is just 66% of that of the latter. Therefore, we cannot predict whether the measures that can improve combustion stability under air atmosphere are still effective and economical when combustion is carried out under oxy-fuel conditions. Hence, the current work will focus on the reasons for the differences in combustion characteristics of porous media under air-fuel and oxy-fuel conditions. In addition to the equivalent ratio, the parameters of porous media materials, including thermal conductivity, pore size, and extinction coefficient, are considered as variables. The

influence of the abovementioned factors on the flame stability and temperature profiles is studied and compared to air-fuel combustion under the same conditions.

2. Materials and methods

2.1. Experimental setup

The primary purpose of the experimental work in this paper is to validate the accuracy of the numerical model. We replicated the burner structure used in the experiment by Gao et al. [15] and applied it to the study of oxy-fuel combustion. The schematic diagram of the experimental device is shown in Fig. 1 (a). A mass flow controller (MFC) with a range of 0–10 SLM and an accuracy of 2% of full scale (2% F.S.) is used for the flow control of CH_4 and O_2, while the MFC with a range of 0–50 SLM is used for CO_2. The fuel and combustion-supporting gas flow through a four-way valve and a 30 cm length of porous medium pipe to ensure adequate mixing of the components. The physical model of the burner is shown in Fig. 1 (b) and Fig. 1 (c). The total length of the burner is 12 cm, the preheating zone and the combustion zone each occupy 6 cm, and the radius is 5 cm. The preheating zone consists of alumina spheres with a diameter of 3 mm, and the combustion zone consists of 10 ppi (pore per inch) SiC foam. To reduce heat loss, the burner wall is wrapped with a layer of 2.5 cm thick refractory fiber. Most of the components in the burner refer to Gao et al. [15]. The thermophysical parameters of the material which were calculated from empirical equations combined with porosity as well as pore size are summarized in Table 1. Since the flashback phenomenon of the burner is also one of the objects of concern in this paper, some potentially dangerous situations need to be prevented. After entering the burner, the premixed gas will pass through a SiC foam layer with a thickness of 2 cm and a pore diameter of 60 ppi. For the convenience of description, this section of SiC porous material is named pre-SiC in the following. On the one hand, the pre-SiC component prevents the tempering flame from entering the gas transportation pipe, and on the other hand, it can improve the velocity uniformity on the inlet of the burner. When flame appears on the surface of pre-SiC, it is proved that the blow-off phenomenon has occurred. At the same time, the heat exchange between pre-SiC and the downstream burner needs to be avoided. Therefore, there is a cavity between the 3 mm packed bed and the direct contact between the two layers of porous media is avoided. As shown in Fig. 1, there are 9 S-type thermocouples (TC1 ~TC9) distributed in a packed bed of 3 mm alumina

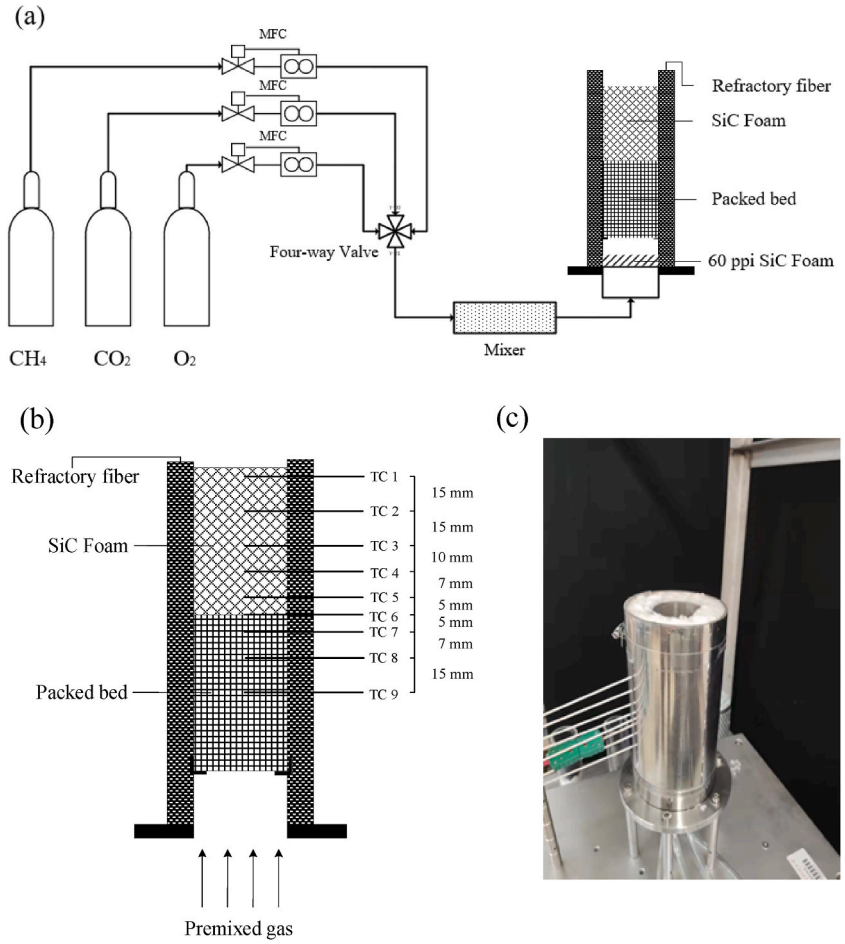

Fig. 1. The schematic diagram of the experimental device: (a) Experimental system; (b) The distribution of thermocouples; (c) PMC burner picture.

Table 1
Physical properties of the porous medium material.

Property	Unit	Preheating zone	Combustion zone
Density	kg/m^3	3900	3200
Heat capacity	J/(kg·K)	910	825
Porosity	–	0.4	0.8
Extinction coefficient	1/m	800	234.1
Thermal conductivity	W/(m·K)	0.28	0.71
Pore diameter	mm	3	2.56

pellets and a 10 ppi SiC foam ceramic layer. Given that the combustion reaction occurs primarily in the combustion zone, where the temperature gradient is the greatest at the interface of the two porous materials, only three thermocouples (TC7∼TC9) are positioned in the preheating zone (3 mm ball). Five thermocouples (TC1∼TC5) are situated in the combustion zone (10 ppi SiC), and one (TC6) is located at the interface. A data collector model (NI cDAQ-9174 and NI 9214) is used to collect temperature data measured by thermocouples.

2.2. Numerical methods

2.2.1. Governing equations

The processes in the burner include gas flow in the porous media, convection heat transfer between the solid and gas phases, solid radiation, solid heat conduction, and all chemical reactions. In this paper, a solver for the simulation of the combustion process in a two-layer porous burner was created based on the open-source CFD software OpenFOAM.

The following principal assumptions were made:

(1) Potential catalytic effects of the high-temperature solid are negligible.
(2) The Dufour effect is negligible.
(3) The mixture gas is non-radiating.

First, the Ergun resistance model was added to the momentum equation in the form of a momentum source term to simulate the pressure drop of the premixed gas in the porous media. The governing equations are expressed as follows:

Continuity equation:

$$\frac{\partial(\varepsilon\rho_g)}{\partial t}+\nabla(\varepsilon\rho_g U)=0 \tag{1}$$

Momentum equation:

$$\frac{\partial(\varepsilon\rho_g U)}{\partial t}+\nabla(\varepsilon\rho_g U\cdot U)=-\nabla P+\nabla(\mu\cdot\nabla U)+S_i \tag{2}$$

where ε is the porosity of the porous media, ρ_g is the density of the premixed gas, and μ is the dynamic viscosity. The resistance source term S_i is defined as [26]:

$$S_i=180\frac{(1-\varepsilon^2)}{\varepsilon^3}\frac{U\cdot u_i}{d^2}+1.8\frac{(1-\varepsilon)}{\varepsilon^3}\frac{\rho_g u_i|U|}{d} \tag{3}$$

Where d is the pore diameter. In equation (3), the pressure drop caused by the fluid flowing through the solid matrix is divided into two categories. The first category represents the viscous resistance, and the second one is the inertial resistance.

Second, a separate energy equation was added to solve the temperature field of the solid matrix, which was coupled with the gas energy equation in the form of an energy source term.

Gas-phase energy equation:

$$\frac{\partial}{\partial t}(\varepsilon\rho_g C_g T_g)+\nabla(U\varepsilon\rho_g C_g T_g)=\nabla(\varepsilon\lambda_g\nabla T_g)-\varepsilon\sum_{i=1}^{N}\omega_i h_i W_i-S \tag{4}$$

Solid-phase energy equation:

$$(1-\varepsilon)\frac{\partial}{\partial t}(\rho_s C_s T_s)=\nabla(\lambda_{eff}\nabla T_s)+S \tag{5}$$

where C and λ are the heat capacity and thermal conductivity, respectively, and ω_i, h_i, and W_i are the molar production rate, molar enthalpy, and molecular weight, respectively, of the *i-th* species. The subscripts g and s denote the gas and solid matrix, respectively. The temperature source term S of the two equations is defined as:

$$S=H_v(T_g-T_s) \tag{6}$$

The above formula indicates the convective heat transfer rate between the gas and solid matrix, and H_v is defined as the volumetric

heat transfer coefficient:

$$H_v = \frac{Nu_v \cdot \lambda_g}{d^2} \tag{7}$$

In the above equation, Nu_v is defined as the volume-based Nusselt number:

In packed beds [27]:

$$Nu = \left\{ \left(1.18\mathrm{Re}^{0.58}\right)^4 + \left[0.23(\mathrm{Re}/\varepsilon)^{0.75}\right]^4 \right\}^{1/4} \quad \left(1 \le \mathrm{Re}/\varepsilon \le 7.7 \times 10^5\right) \tag{8}$$

In foams [28]:

$$Nu_v = 0.819[1 - 7.33(d/L)]\mathrm{Re}^{0.36[1+15.5(d/L)]} \quad (5.1 \le \mathrm{Re} \le 564, 0.005 < d/L < 0.136) \tag{9}$$

Where L is the thickness of the solid matrix and Re is the Reynolds number with the pore diameter as the characteristic length.

Due to the complex internal structure of porous media, it is difficult to calculate the radiation heat transfer occurring in pores. As an alternative, the radiation diffusion model has been employed to simulate the radiation heat transfer process in the solid matrix [29]. More concretely, the model simplifies the radiative heat transfer process into a form similar to heat conduction. In equation (5), λ_{eff} is the equivalent thermal conductivity, which consists of two parts:

$$\lambda_{eff} = \lambda_s + \lambda_{rad} \tag{10}$$

where λ_{rad} is the radiant thermal conductivity and is defined as:

$$\lambda_{\mathrm{rad}} = \frac{16\sigma T_s^{\,3}}{3k} \tag{11}$$

where k is the radiative extinction coefficient, obtained from Howell [30], and it is given by:

$$k = \frac{3}{d}(1 - \varepsilon) \tag{12}$$

The model is valid for pore diameters larger than 0.6 mm. Therefore, the final form of the solid phase energy equation is:

$$(1 - \varepsilon)\frac{\partial}{\partial t}(\rho_s C_s T_s) = \nabla((\lambda_s + \lambda_{rad})\nabla T_s) + H_v(T_g - T_s) \tag{13}$$

There is no need to modify the species transport equation:

$$\frac{\partial(\rho Y_i)}{\partial t} + \nabla(\rho V Y_i) = \omega_i W_i \tag{14}$$

Where Y_i and V are the mass fraction and diffuse velocity, respectively, of the *i-th* species. In order to obtain the composition distribution of the temperature field as accurately as possible, the CH_4 skeletal kinetic mechanism (24 species, 155 reactions) is adopted [31].

The ideal gas equation of state is adopted to calculate the density:

$$\rho_g = \frac{\overline{W}P}{RT_g} \tag{15}$$

In the above equation, $\overline{W}$ is the average molar mass of the mixture gas, and R is the universal gas constant.

The OpenFOAM solver is based on an unsteady PISO algorithm with two pressure correctors and two momentum correctors per time step and convergence criteria for residuals 10^{-6}. The time step was selected to be approximately 10^{-4} s with a corresponding Courant (CFL) number of 0.3. The discretization scheme for the unsteady term is an implicit Euler scheme which is first-order bounded. Gauss limited linear schemes were used for the convective terms. Gauss linear orthogonal schemes were used for diffusion terms. Laminar flow is considered to be the flow state of premixed gas inside the porous matrix [22]. However, in OpenFOAM, the basic chemical solver reactingFoam, some assumptions used in the prediction of the species diffusion coefficient may not be appropriate [32]. Therefore, we ported the code to laminarPimpleSMOKE based on OpenSMOKE++ for simulating laminar reaction with detailed mechanisms. The native OpenSMOKE++ ODE (Ordinary Differential Equations) solver which is based on variable-coefficient backward differentiation formula (BDF) methods, is used for complex chemistry integration. The maximum temperature and the position of the flame surface are monitored as a reference for reaching steady-state. Due to the large thermal inertia of the solid matrix, the stable condition requires approximately 15 min.

2.2.2. Boundary conditions

The following boundary conditions of the 2D model were adopted for the gas, solid, and species:

Inlet (x = 0 cm):

$$T_g = T_{g,inlet} = 300K \tag{16}$$

$$(1-\varepsilon)\lambda_{eff}\frac{\partial T_s}{\partial x} = 0 \tag{17}$$

$$Y_i = Y_{i,inlet}, i = 1, 2, \cdots N \tag{18}$$

$$\begin{cases} u = u_{inlet} \\ v = 0 \end{cases} \tag{19}$$

Outlet (x = 12 cm):

$$\frac{\partial T_g}{\partial x} = 0 \tag{20}$$

$$(1-\varepsilon)\lambda_{eff}\frac{\partial T_s}{\partial x} = -\varphi\sigma\left(T_s^4 - T_0^4\right) \tag{21}$$

$$\frac{\partial Y_i}{\partial x} = 0, i = 1, 2, \cdots N \tag{22}$$

$$\frac{\partial u}{\partial x} = \frac{\partial v}{\partial x} = 0 \tag{23}$$

Where $T_0 = 300$ K is the ambient temperature, φ is the emissivity of the solid matrix, and σ is the Stefan Boltzmann constant (5.67×10^{-8} W/(m^2·K^4)). The ratio of O_2/CO_2 was fixed at 0.21/0.79 under oxy-fuel conditions, which is consistent with the O_2 fraction in air. Velocity inlet and pressure outlet are adopted as boundary conditions at the burner inlet and outlet, respectively. The axisymmetric boundary conditions (y = 0 cm) and wedge boundary conditions (z-direction) are adopted by the 2D model. The heat loss on the side wall (y = 2.5 cm) of the burner is a future consideration but not the research object of this work. Therefore, the adiabatic boundary condition is adopted.

2.3. Model validation

Firstly, the number of grids in the model was tested. The results show that all of the maximum numerical errors of the temperature field under the grid numbers 2480, 6780, and 13,600 relatives to grid number 24800 is not exceed 2%. However, in terms of flame

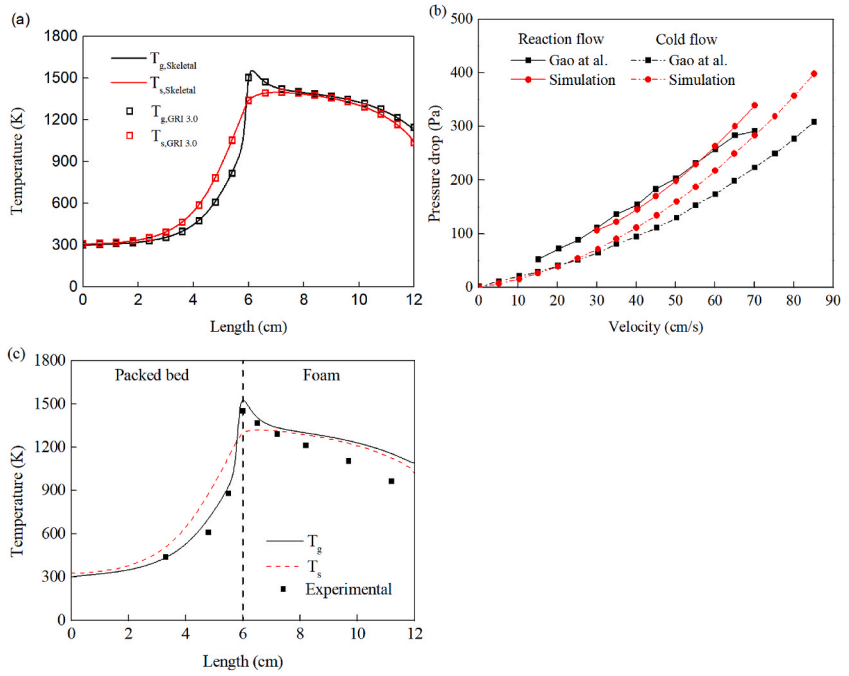

Fig. 2. Model validation: comparison of temperature field between skeleton mechanism and GRI 3.0 (a); comparison of the pressure drop (b); comparison of temperature field with experimental data (c).

propagation speed, there is a difference of 1 cm/s between the grid numbers 6780 and 24,800. Therefore, in order to ensure sufficient accuracy and reduce the calculation cost, grid number 13600 will be used in subsequent calculations. Secondly, Fig. 2 (a) depicts the comparison of the temperature field between the skeletal mechanism and the GRI 3.0. The maximum error is less than 2%, but the CPU time is 1/3 of the latter.

The applied numerical model was validated via comparison to the experimental data. In the first step, since the pressure drop of the burner was not measured in this work, it was compared with the experimental results provided by Gao et al. [15] on premixed air/methane combustion. In the experimental operating parameters, the inlet velocity is 10 cm/s, and the equivalence ratio is 0.6. The results include cold and reaction flow under air-fuel conditions. As shown in Fig. 2 (b), the burner structure and material properties in the experiment are consistent with those used in this work. It was found from the results that the Ergun resistance model used in this paper is in good agreement with the experimental data, especially under reaction flow, and the maximum error was 7.6%. Secondly, the oxy-fuel temperature fields are compared with the experimental data provided by this work. As shown in Fig. 2 (c), it is evidence that the data obtained by the thermocouple in the combustion zone is lower than the calculated value, and the maximum deviation is 15% at the position of TC1. The main reasons for the error are as follows: 1) The diameter of the thermocouple ceramic tube used in this work is 2 mm, which is close to the hole diameter of the porous material. The placement of the thermocouple will inevitably affect the flow field, which may accelerate or decrease the flow velocity at this position; 2) Although a layer of 2.5 cm thick refractory fiber is used to insulate the burner, the heat loss on the tube shell is still considerable. Record through K-type thermocouple, the maximum shell temperature the downstream of the burner is reached ~400 K. The heat loss through convection, and thermal radiation accounts for more than 13% of the burner's thermal load under this working condition; 3) Some scholars have pointed out that the temperature collected by the thermocouples with bare junction will indeed be lower than the actual gas temperature. In the study of Zheng et al. [33], due to the radiant heat loss of the thermocouple, the gas temperature in the combustion zone was 30–90 K higher than the temperature collected by thermocouples. Based on the above considerations, it is considered that it is feasible to employ the current numerical model to predict the actual situation.

3. Results and discussion

3.1. Overall performance

Generally, three types of flame states exist in two-layer porous media burners: 1) flash-back, 2) stable flame and 3) blow-off. The state of flash-back and blow-off is unstable and potentially dangerous, and it is difficult to be utilized in a two-layer burner. The characteristic of the stable flame state is that the flame can be stabilized at the interface of the two layers of the porous matrix. However, there is almost no observation that the position of the flame peak temperature is just at the interface (x = 6 cm) in our simulation work but close to its upstream or downstream position. Especially in the combustion zone, the flame may be located at a position far from the interface and close to the outlet but will not blow out. This phenomenon may be caused by heat loss at the outlet boundary. This situation creates complexity for the analysis of stable combustion conditions. Therefore, we define a new stable flame condition, that is, when the flame front surface is located at a distance of ±0.5 cm from the interface. At the same time, the flame surface is also defined. In OpenFOAM, Qdot represents the total heat release rate of a chemical reaction. It is stipulated here that the position of 1% of maximum Qdot is the front and back edge of the flame. As shown in Fig. 3, as the inlet velocity increases, the flame front moves downstream and just touches the interface. It is considered that the down limit of the inlet flow velocity is reached. The corresponding condition is the minimum velocity (V_{min}) of the stable range. Similarly, the upper limit velocity (V_{max}) refers to when the flame front just leaves the interface and continues to move downstream. As observed from our calculation results, the thickness of the flame front under this definition is about 5 mm. According to this definition, a flame front is only considered to be in a stable state if it is within ±5 mm of the interface. This is different from the results of Gao et al. [15], where the peak temperature was located far

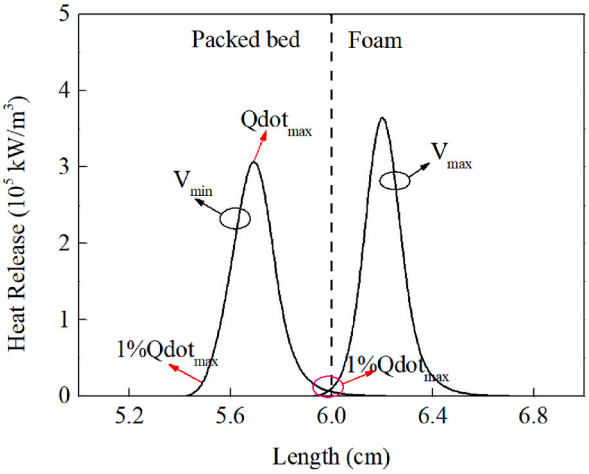

Fig. 3. Schematic of the flame stable range.

away from the interface between the two solid matrixes in some operating conditions. We considered the flame stable as long as it was not blown out in this experiment. Due to the description of the stale flame state in this paper being more demanding, the calculation results of V_{max} are inconsistent with the experimental data of Gao et al. [15].

Table 2 and Table 3 show the free flame propagation velocity, adiabatic combustion temperature, and CO emissions under oxy-fuel and air-fuel conditions (the results are obtained by ANSYS Chemkin Pro). It can be seen that there are significant differences in all indicators, which are consistent with the results of PMC (Table 4). In almost any case, the oxy-fuel stable range of PMC is only approximately 50% of that under air-fuel conditions. Due to the stable conditions required for combustion with various combustion-supporting gases being different, comparisons cannot be made at the same equivalence ratio and inlet velocity. However, considering the boundary conditions of the burner sidewall surface, there is no heat loss, which is similar to adiabatic combustion conditions. Thus, the case of a 0.6 equivalence ratio and flames just remaining at the interface is chosen to illustrate the difference in combustion characteristics. The corresponding inlet velocity is 8 cm/s under oxy-fuel conditions and 25 cm/s under air-fuel conditions. As shown in Fig. 4 (a), obviously, the peak flame temperature under the oxy-fuel conditions is ~300 K lower than that under the air-fuel conditions. As a result, the combustion conditions are worse than those under air-fuel conditions. However, considering that the combustion temperature under air-fuel conditions is close to 1800 K, porous medium materials often have a low heat resistance (for example, the maximum useable temperature of SiC ceramics usually does not exceed 1800 K), and they cannot be employed for long periods at high temperatures [34]. Therefore, the low flame temperature under oxy-fuel conditions may be more suitable for the application of porous media combustion. In addition, the increase in the O_2 fraction in the combustion-supporting gas increases the flame temperature, and it is inferred that the stable range could also be broadened or shifted by adjusting the O_2/CO_2 ratio. Since H_2 and CO are the most important intermediate products in methane combustion, their fractions at the flame front are shown in Fig. 4 (b). The CO_2 in the combustion-supporting gas participates in a chemical reaction, resulting in a higher CO concentration than in air-fuel conditions.

There are two reasons for the significant difference between oxy-fuel and air-fuel conditions. 1) The physical properties of CO_2 and air, such as density, heat capacity, and thermal conductivity, are significantly different, which may affect flame temperature and propagation speed. 2) As a product of the chemical reaction, the CO_2 fraction will play an important role in the rate of the chemical reaction. The CO_2 participates in the chemical reaction by converting back to CO. However, CH_4 blending with the resulting CO would diminish the burning velocity. In order to verify the priority of the factors mentioned above, an inert artificial species FCO_2 is introduced to replace CO_2 in the premixed gas. The FCO_2 has the same physical properties as CO_2, but it is an inert gas and will not participate in any chemical reactions. Fig. 6 shows the temperature fields under CO_2 and FCO_2 atmospheres when the inlet velocity is 9 cm/s and 10 cm/s (equivalence ratio = 0.6), respectively.

As shown in Fig. 5 (a), the temperature fields are basically the same, and there is only a 13 K difference in the peak temperature. The emission of CO under FCO_2 conditions is 0.1 ppm, and under CO_2 conditions is 2.4 ppm. However, the CO_2 atmosphere will have a slight effect on the flame propagation velocity, consequently a little difference in the stale range. As shown in Fig. 5 (b), the flame under the CO_2 condition has entered the downstream of the burner while the flame of FCO_2 remains at the original position. The results show that the stable range under FCO_2 conditions is 5–10 cm/s, while CO_2 is 5–9 cm/s. Therefore, it can be shown that the chemical properties of CO_2 have no significant effect on the flame temperature. Instead, high concentrations of CO_2 may have led to competition for the H in the radical chain branching, which slightly affected the flame speed.

3.2. *Influence of the porous medium matrix on the flame stability*

It is found, based on the calculation model, that physical parameters such as the pore diameter, porosity, and thermal conductivity of the porous matrix impact the temperature field. Moreover, especially in ceramic foams, the pore diameter and thermal conductivity are tough to measure accurately. However, the pore diameter plays a crucial role in the calculation of the Reynolds number and volumetric heat transfer coefficient. Therefore, the measurement error of this parameter may be the main error source in the calculation results. Many researchers have studied the effect of porous media material parameters on the stable range under air-fuel conditions, and the conclusion has been clear. However, as mentioned above, PMC improves the stability and efficiency of oxy-fuel combustion. Need to verify that the adjustments of the material under oxy-fuel conditions are effective and economical. For those reasons, it is necessary to make a quantitative comparison with the calculated results under air-fuel conditions. Thus, based on the model, the influence of the thermal conductivity, convective heat transfer coefficient and extinction coefficient on the stable range and temperature field are studied in the following section.

3.2.1. *Conductivity*

To clearly illustrate the influence of the porous medium matrix on the combustion process, a thermal resistance model is established, as shown in Fig. 6. The model indicates that the solid matrix absorbs high-temperature gas waste heat from the combustion

Table 2
The free flame combustion characteristics under the oxy-fuel condition.

Equivalence ratio	Free flame propagation speed (cm/s)	Adiabatic temperature (K)	CO (ppm)
0.6	0.4	1262	0.4
0.65	1.3	1341	1.3
0.7	2	1393	3.3
0.75	3	1455	10
0.8	3.5	1516	31

Table 3
The free flame combustion characteristics under the air-fuel condition.

Equivalence ratio	Free flame propagation speed (cm/s)	Adiabatic temperature (K)	CO (ppm)
0.6	15.7	1653	8.5
0.65	19.8	1743	26.9
0.7	24.7	1830	77
0.75	28.7	1913	197
0.8	32.6	1989	458

Table 4
Effect of the equivalence ratio on the stable range.

Equivalence ratio	Air-fuel (cm/s)			Oxy-fuel (cm/s)		
	V_{min}	V_{max}	Range	V_{min}	V_{max}	Range
0.55	18	27	9	4	8	4
0.6	20	30	10	5	9	4
0.65	24	35	11	7	11	4
0.7	27	38	11	8	12	4
0.75	31	42	11	9	14	5
0.8	33	46	13	10	15	5

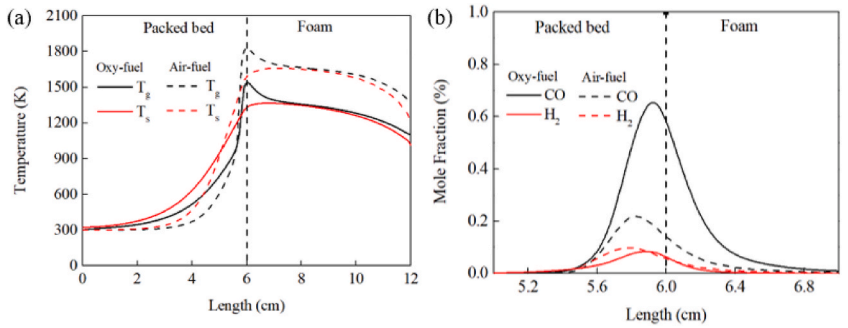

Fig. 4. Comparison of oxy-fuel and air-fuel conditions: temperature field (a), species (b).

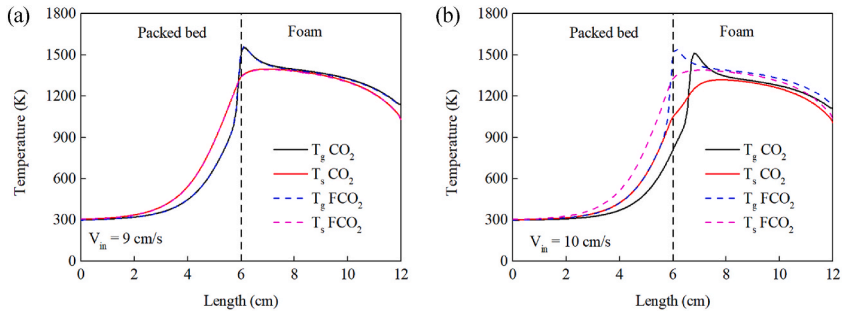

Fig. 5. Comparison of temperature fields: V_{in} = 9 cm/s (a); V_{in} = 10 cm/s (b).

zone, transfers it upstream through conduction and radiation, and finally preheats the unburned gas. R1 is the convective heat transfer resistance between the premixed gas and solid matrix in the preheating zone, R2 is the thermal conductivity resistance in the preheating zone, R3 is the thermal radiation resistance in the preheating zone, R4 and R5 are the thermal conductivity and thermal radiation resistances, respectively, in the combustion zone, and R6 is the convective heat transfer resistance in the combustion zone. R1 and R6 are determined by the volumetric heat transfer coefficient of each section, R2 and R4 are determined by the thermal conductivity of the material, and R3 and R5 are determined by the extinction coefficient and temperature. When R2 increases with decreasing thermal conductivity of the preheating zone materials (λ_{up}), the total thermal resistance of the system increases, which results in more difficult heat transfer from downstream to upstream. Thus, the preheating rate of the premixed gas by the porous matrix decreases, and the flame propagation speed decreases, resulting in a relatively low V_{min}. Moreover, it is easy to infer that the change in upstream heat transfer conditions also affects V_{max}. When the inlet flow velocity is gradually increased, the flame enters the

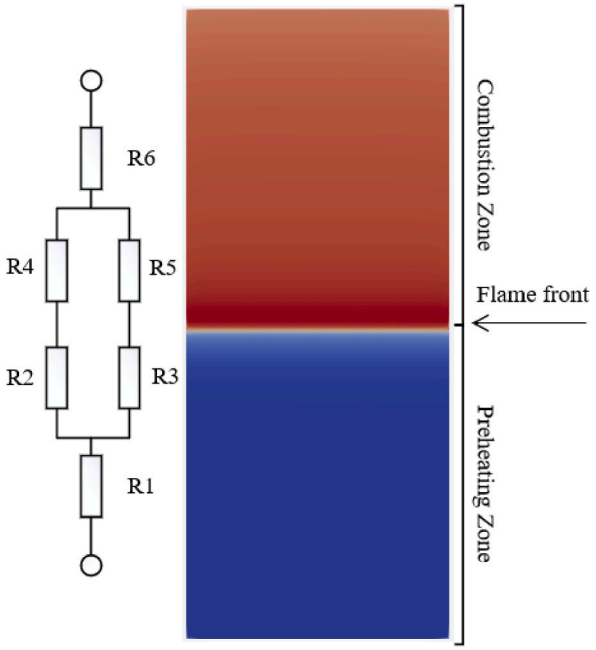

Fig. 6. Schematic of the thermal resistance.

downstream region. The unburned gas obtains less heat in the preheating zone, resulting in a relatively low temperature after entering the downstream region, which leads to a slight decrease in the flame propagation speed. The final result is a small decrease in both V_{min} and V_{max}.

In contrast, increasing λ_{up} reduces R2 will increase V_{min} and V_{max}. In addition, Table 5 indicates that whether λ_{up} is increased or decreased by 1 time, the effect on the stability range seems to be nonsignificant. If the thermal conductivity is increased 5 times or 10 times, R2 is greatly reduced, causing the value of V_{min} to gradually approach V_{max}, so the stable range is reduced. The results of a similar study by Barra et al. [23] are also presented in Table 5. It can be seen that the trend of the stable limit in this paper is the same as their data, but differs greatly in value. There are two possible reasons for the differences between the results. First, the porous matrix material used for their burner is different from that of this paper, especially in the preheating zone, where ceramic foams were also employed in the work of Barra et al. [23]. Second, the definition of steady combustion in the current work seems to be more stringent than that of Barra's. In this paper, the flame thickness is approximately 5 mm, and the condition is recognized as stable combustion only when the flame front is located at the interface.

As indicated in Table 6, although the thermal conductivity of the downstream material (λ_{down}) changes, there is little effect on V_{min}. This occurs because the temperature in the combustion zone is relatively high, and radiation heat transfer in this area is dominant. Since the λ_{rad}/λ_s is more than 5 in the combustion zone, the change of R4 imposes little effect on the thermal resistance of the system. As a result, the preheating rate of the upstream premixed gas does not change significantly, and the impact on V_{min} is limited. When the flame enters the downstream area due to the increase in inlet velocity, the downstream material continues to preheat the unburned gas.

Table 5
Effect of the conductivity of the preheating zone on the stable range.

Equivalence ratio	Conductivity	Air-fuel (cm/s)			Oxy-fuel (cm/s)		
		V_{min}	V_{max}	Range	V_{min}	V_{max}	Range
0.6	$1\lambda_{up}/1\lambda_{down}$	20	30	10	5	9	4
	$0.5\lambda_{up}/1\lambda_{down}$	19	29	10	5	10	5
	$2\lambda_{up}/1\lambda_{down}$	22	32	10	6	10	4
	$5\lambda_{up}/1\lambda_{down}$	28	38	10	8	12	4
	$10\lambda_{up}/1\lambda_{down}$	35	41	7	9	12	3
0.7	$1\lambda_{up}/1\lambda_{down}$	27	38	11	8	12	4
	$0.5\lambda_{up}/1\lambda_{down}$	25	36	11	7	11	4
	$2\lambda_{up}/1\lambda_{down}$	29	40	11	9	13	4
	$5\lambda_{up}/1\lambda_{down}$	37	44	7	11	15	4
	$10\lambda_{up}/1\lambda_{down}$	46	49	3	14	15	1
0.65	$1\lambda_{up}/1\lambda_{down}$	48	74	26	–	–	–
Barra et al. [23]	$10\lambda_{up}/1\lambda_{down}$	65	74	9	–	–	–

Table 6
Effect of the combustion zone conductivity on the stable range.

Equivalence ratio	Conductivity	Air-fuel (cm/s)			Oxy-fuel (cm/s)		
		V_{min}	V_{max}	Range	V_{min}	V_{max}	Range
0.6	$1\lambda_{up}/1\lambda_{down}$	20	30	10	5	9	4
	$1\lambda_{up}/0.5\lambda_{down}$	20	29	9	5	10	5
	$1\lambda_{up}/2\lambda_{down}$	20	33	13	5	10	5
	$1\lambda_{up}/5\lambda_{down}$	20	35	15	5	12	7
	$1\lambda_{up}/10\lambda_{down}$	20	36	16	5	13	8
0.7	$1\lambda_{up}/1\lambda_{down}$	27	38	11	8	12	4
	$1\lambda_{up}/0.5\lambda_{down}$	27	36	9	8	11	3
	$1\lambda_{up}/2\lambda_{down}$	27	40	13	8	13	5
	$1\lambda_{up}/5\lambda_{down}$	27	42	15	8	14	6
	$1\lambda_{up}/10\lambda_{down}$	27	43	16	8	15	7
0.65	$1\lambda_{up}/1\lambda_{down}$	48	74	26	–	–	–
Barra et al. [23]	$1\lambda_{up}/10\lambda_{down}$	48	92	44	–	–	–

Because λ_{down} increases, the preheating rate increases, which leads to a relatively high flame propagation speed and a small increase in V_{max}, so the stable range expands.

The variation in the gas-phase temperature field with the thermal conductivity under oxy-fuel conditions is shown in Fig. 7. The inlet velocity is 8 cm/s, and the equivalence ratio is 0.6. It is observed that the change in λ_{up} imposes no major effect on the peak temperature but imposes a significant influence on the upper limit of the temperature range. With increasing λ_{up}, the flame propagation speed increases, and the flame tends to move upstream. The change in λ_{down} seems to impose a little effect on the temperature field, but with increasing thermal conductivity, the downstream temperature gradient slightly increases. Comparing the oxy-fuel and air-fuel conditions, since the gas flow rate is relatively low, the stable range is relatively narrow. Especially when the upstream thermal conductivity is increased 10 times, the change of stable range is no longer observed under oxy-fuel conditions.

3.2.2. Volume heat transfer coefficient

The thermal resistance model can also be applied to determine the influence of the pore diameter on stability. However, it should be noted that the change in pore diameter affects the calculation of both the volumetric heat transfer coefficient and extinction coefficient. Since the volumetric heat transfer coefficient is obtained according to an empirical equation, many researchers have obtained different empirical equations through experiments. However, the volumetric convective heat transfer coefficients obtained according to these equations exhibit certain differences. For example, in terms of the combustion zone material parameters in this paper, the H_v value calculated with the model of Younis et al. [28] is 29,400 ($W/m^3{\cdot}K$) for a Reynolds number of 20, while the value calculated based on Fu et al. [35] is 16,500 ($W/m^3{\cdot}K$), with a difference of 43.9%. In this section, the effect of the volumetric heat transfer coefficient on the results is separately studied. The effect of the change in the pore diameter on the extinction coefficient is not considered temporarily.

Equation (7) indicates that a small pore diameter results in an enormous H_v value, which implies that the heat transfer resistance between the premixed gas and the solid matrix is low. The heat exchange between the unburned gas and solid matrix is notable, resulting in the ignition temperature being reached within a relatively short time. Therefore, it is inferred that reducing the pore size of either the preheating zone or the combustion zone enhances flame propagation and increases V_{min}. Conversely, increasing the pore size reduces V_{min}. Moreover, the upstream preheating rate also affects the downstream chemical reaction rate, resulting in V_{max} exhibiting the same trend. The calculation results are listed in Table 7.

When reducing the pore diameter of the combustion zone (d_{down}), the total heat transfer resistance of the system is also reduced. When the flame enters the downstream region, the heat transfer to the unburned gas in the combustion zone increases, resulting in relatively fast flame propagation, and V_{max} increases accordingly. Moreover, it is found that the change in d_{down} also exerts a major impact on V_{min}. It is concluded that compared to the thermal conductivity of the material, the change in the thermal resistance of the system via the pore size is more profound. Hence, the convective heat transfer thermal resistance may be the most important aspect of the total thermal resistance of the burner system.

The variation in the gas-phase temperature field with the volume heat transfer coefficient under oxy-fuel conditions is shown in Fig. 8, while the boundary conditions are the same as in Fig. 9. It is evident from Fig. 8 (a) that with increasing pore diameter, the flame gradually moves downstream. As shown in Fig. 8 (b), the peak temperature increases with increasing pore diameter. Specifically, the peak temperature of $2d_{down}$ is 115 K higher than that of $0.5d_{down}$. The reason is that the increase in the pore diameter reduces the volume heat transfer coefficient and decreases the speed of heat transfer from the gas phase to the solid phase.

3.2.3. Extinction coefficient

In the numerical model, radiation heat transfer is simplified as a process similar to heat conduction. The radiant thermal conductivity may be regarded as a diffusion coefficient that greatly changes with the temperature. Therefore, the influence of the radiant thermal conductivity on the flame stability should be consistent with the trend due to the material thermal conductivity. Equation (11) indicates that the result of reducing the extinction coefficient k is an increase in λ_{cad}. Consequently, it is inferred that reducing k increases both V_{min} and V_{max}. Conversely, increasing k produces the opposite result. Table 8 summarizes the calculation results obtained

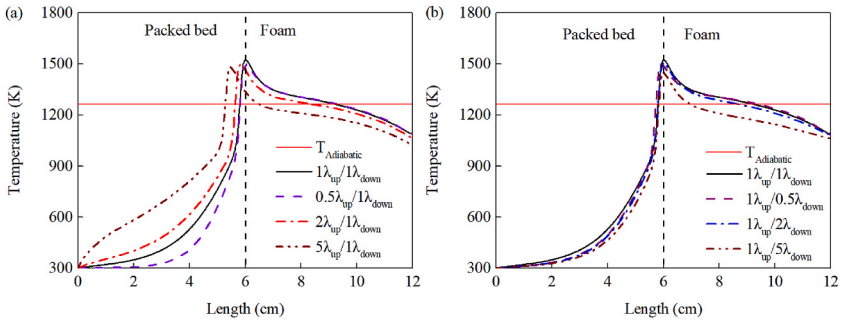

Fig. 7. Axis temperature field changes with the thermal conductivity, λ_{up} (a), λ_{down} (b).

Table 7
Effect of the volume heat transfer coefficient on the stable range.

Equivalence ratio	Volume heat transfer coefficient	Air-fuel (cm/s)			Oxy-fuel (cm/s)		
		V_{min}	V_{max}	Range	V_{min}	V_{max}	Range
0.6	$1d_{up}/1d_{down}$	20	30	10	5	9	4
	$0.5d_{up}/1d_{down}$	26	36	11	7	13	6
	$2d_{up}/1d_{down}$	18	28	10	6	10	4
	$1d_{up}/0.5d_{down}$	21	45	24	6	15	9
	$1d_{up}/2d_{down}$	20	25	5	5	8	3
0.7	$1d_{up}/1d_{down}$	27	38	11	8	12	4
	$0.5d_{up}/1d_{down}$	35	44	9	10	15	5
	$2d_{up}/1d_{down}$	27	33	6	7	11	4
	$1d_{up}/0.5d_{down}$	32	55	23	16	30	14
	$1d_{up}/2d_{down}$	26	29	3	7	9	2
0.65	$1d_{up}/1d_{down}$	48	74	26	–	–	–
Barra et al. [23]	$0.5d_{up}/0.5d_{down}$	55	82	27	–	–	–
	$1d_{up}/0.5d_{down}$	52	82	30	–	–	–
	$2d_{up}/2d_{down}$	40	64	24	–	–	–

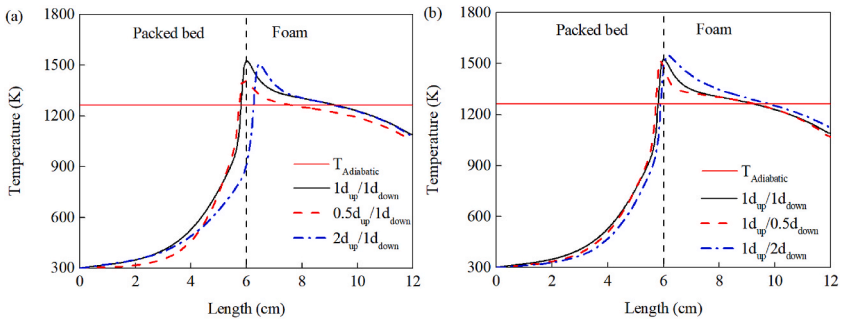

Fig. 8. Temperature field changes with the volume heat transfer coefficient, d_{up} (a), d_{down} (b).

by changing the extinction coefficient of the preheating zone (k_{up}) and combustion zone (k_{down}). In addition, it is observed that the influence of the change in the *k* value of the combustion zone on V_{min} remains nonsignificant. Only V_{min} exhibits a slightly decreasing trend with increasing downstream *k* value.

In regard to the temperature field, as shown in Fig. 9 (a) and (b), the change in k_{up} seemingly yields no effect on the downstream temperature distribution, and the same applies to k_{down}. It seems that the change in the extinction coefficient imposes little effect on the peak temperature and outlet temperature.

4. Conclusions

In this paper, a two-layer porous media combustion model was established. The combustion behaviour under oxy-fuel and air-fuel conditions were compared. Through the analysis of the thermal resistance model, it can be inferred that the influence of the variables, including the equivalence ratio, thermal conductivity, volume heat transfer coefficient and extinction coefficient on the stable range and temperature field, is consistent under oxy-fuel and air-fuel conditions. The results reveal that:

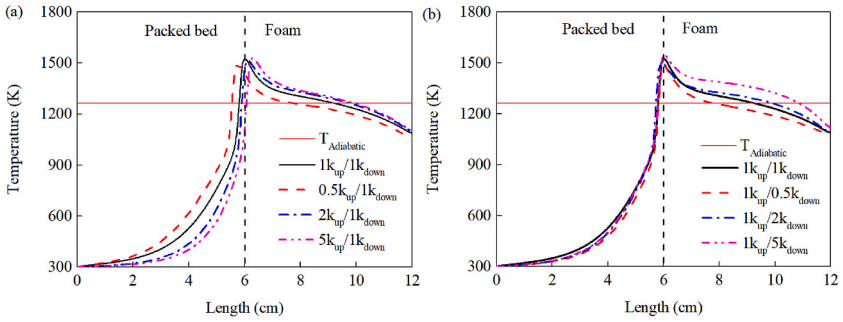

Fig. 9. Temperature field changes with the extinction coefficient, k_{up} (a), k_{down} (b).

Table 8
Effect of the extinction coefficient on the stable range.

Equivalence ratio	Extinction coefficient	Air-fuel (cm/s)			Oxy-fuel (cm/s)		
		V_{min}	V_{max}	Range	V_{min}	V_{max}	Range
0.6	$1k_{up}/1k_{down}$	20	30	10	5	9	4
	$0.5k_{up}/1k_{down}$	24	33	9	6	10	4
	$2k_{up}/1k_{down}$	19	30	11	5	9	4
	$5k_{up}/1k_{down}$	19	30	11	5	9	4
	$1k_{up}/0.5k_{down}$	21	34	13	6	11	5
	$1k_{up}/2k_{down}$	21	29	8	5	9	4
	$1k_{up}/5k_{down}$	19	26	7	5	8	3
0.7	$1k_{up}/1k_{down}$	27	38	11	8	12	4
	$0.5k_{up}/1k_{down}$	32	40	8	9	12	3
	$2k_{up}/1k_{down}$	25	37	12	7	11	4
	$5k_{up}/1k_{down}$	25	36	11	7	11	4
	$1k_{up}/0.5k_{down}$	28	43	15	8	12	4
	$1k_{up}/2k_{down}$	28	34	6	8	11	3
	$1k_{up}/5k_{down}$	27	30	3	8	10	2
0.65 Barra et al. [23]	$1k_{up}/1k_{down}$	48	74	26	–	–	–
	$1/6k_{up}/1k_{down}$	57	75	18	–	–	–
	$6k_{up}/1k_{down}$	40	72	32	–	–	–
	$1k_{up}/1/6k_{down}$	34	57	23	–	–	–

(1). The difference in physical properties between CO_2 and air is the main reason for the significant variation of combustion behaviours under the conditions of oxy-fuel compared to air-fuel. The specific performance is characterised by a reduced combustion temperature and a slower flame propagation speed. For example, at an equivalence ratio of 0.6, the combustion temperature under oxy-fuel conditions is approximately 300 K lower than that under air-fuel conditions. Moreover, in almost any case, the stable range is only approximately 50% of that of the latter. However, considering that porous medium materials tend to have relatively low heat resistance and low operating temperature, a low flame temperature may be more conducive to the application of porous media combustion.

(2). Any structural changes that reduce the internal heat transfer resistance of porous media, for example, increasing the thermal conductivity of the material or the volume heat transfer coefficient and reducing the extinction coefficient, increase the minimum and maximum stable velocities. Increasing the thermal resistance produces the opposite effect.

(3). Even if the thermal conductivity and extinction coefficient values are increased by 5 times, their impact on broaden the stable range is not significant. However, reducing the pore size of the combustion zone by 50% will increase the stable range by more than 100%.

Author contributions

Conceptualization: Zhu He.
Methodology: Mingjian Liao.
Validation: Zhu He.
Resources: Xuecheng Xu, Zhu He, Shuyuan Jia, Xiong Liang , Yawei Li, Tat Leung Chan and Ting Liu.
Writing — original draft preparation: Mingjian Liao.
Writing — review and editing: Zhu He, Ting Liu.

Declaration of competing interest

The authors declare that they have no known competing financial interests or personal relationships that could have appeared to influence the work reported in this paper.

Data availability

No data was used for the research described in the article.

Acknowledgments

This work was financially supported by the National Natural Science Foundation of China [Grant numbers. U22A20127], the Special Project of Central Government for Local Science and Technology Development of Hubei Province [Grant numbers. 2019ZYYD003 , 2019ZYYD076], the Central Research Grant (Project No. 4-BCD3) and the Mechanical Engineering Department (Project No. 88Y9) of The Hong Kong Polytechnic University.

References

[1] D. José, Figueroa, Fout Timothy, Plasynski Sean, Advances in CO_2 capture technology—the U.S. Department of energy's carbon sequestration program, Int. J. Greenh. Gas Control (2008).
[2] D. Gilfillan, G. Marland, CDIAC-FF: global and national CO_2 emissions from fossil fuel combustion and cement manufacture: 1751-2017, Earth Syst. Sci. Data Discuss. 2020 (2020) 1–23.
[3] Cebrucean Dumitru, Cebrucean Viorica, Ionel Ioana, CO_2 capture and storage from fossil fuel power plants, Energy Proc. (2014).
[4] P. Gladysz, W. Stanek, L. Czarnowska, S. Sladek, A. Szick, Thermo-ecological evaluation of an integrated MILD oxy-fuel combustion power plant with CO_2 capture, utilisation, and storage – a case study in Poland, Energy 144 (2018) 379–392.
[5] F. Wu, M.D. Argyle, P.A. Dellenback, M.H. Fan, Progress in O_2 separation for oxy-fuel combustion-A promising way for cost-effective CO2 capture: a review, Prog. Energy Combust. Sci. 67 (2018) 188–205.
[6] H. Wu, Y. Mao, Z. Liu, Y. Zhang, H. Liao, Numerical simulation of oxy-fuel combustion characteristics in a 200 MWe coal-fired boiler, Greenhouse Gases Ence Technol. 9 (2019).
[7] F. Sher, M.A. Pans, C. Sun, C. Snape, H. Liu, Oxy-fuel combustion study of biomass fuels in a 20 kWth fluidized bed combustor, Fuel 215 (2018) 778–786.
[8] Z. Zhang, B. Lu, L. Zhang, X. Li, C. Luo, Y. Xu, Z. Zhao, C. Zheng, Computational study on the effect of gasification reaction on pulverized coal MILD combustion diluted by N_2 and CO_2, Appl. Therm. Eng. 158 (2019), 113806.
[9] M. Ilbas, A. Bektas, S. Karyeyen, A new burner for oxy-fuel combustion of hydrogen containing low-calorific value syngases: an experimental and numerical study, Fuel 256 (2019), 115990.115991-115990.115914.
[10] M.A. Mujeebu, M.Z. Abdullah, A.A. Mohamad, M.Z. Abu Bakar, Trends in modeling of porous media combustion, Prog. Energy Combust. Sci. 36 (2010) 627–650.
[11] M.A. Mujeebu, A.A. Mohamad, M.Z. Abdullah, Applications of porous media combustion technology - ScienceDirect, Role Colloidal Syst. Environ. Protect. (2014) 615–633.
[12] H.B. Gao, Z.G. Qu, X.B. Feng, W.Q. Tao, Combustion of methane/air mixtures in a two-layer porous burner: a comparison of alumina foams, beads, and honeycombs, Exp. Therm. Fluid Sci. 52 (2014) 215–220.
[13] S.M. Hashemi, S.A. Hashemi, Flame stability analysis of the premixed methane-air combustion in a two-layer porous media burner by numerical simulation, Fuel 202 (2017) 56–65.
[14] H. Liu, B.W. Li, H.L. Wang, Experimental study of multispecies gas combustion in a several-section porous media burner, Combust. Explos. Shock Waves 50 (2014) 150–157.
[15] H.B. Gao, Z.G. Qu, X.B. Feng, W.Q. Tao, Methane/air premixed combustion in a two-layer porous burner with different foam materials, Fuel 115 (2014) 154–161.
[16] C.E. Arrieta, A.M. García, A.A. Amell, Experimental study of the combustion of natural gas and high-hydrogen content syngases in a radiant porous media burner, Int. J. Hydrogen Energy (2017). S0360319917310029.
[17] E.K. Quaye, J. Pan, Q. Lu, Y. Zhang, Y. Wang, A.A. Alubokin, Study on combustion characteristics of premixed methane-oxygen in a cylindrical porous media combustor, Chem. Eng. Proc. Process Intensificat. 159 (2021), 108207.
[18] M.V. Heitor, A.L.N. Moreira, Thermocouples and sample probes for combustion studies, Prog. Energy Combust. Sci. 19 (1993) 259–278.
[19] I. Yakovlev, S. Zambalov, Three-dimensional pore-scale numerical simulation of methane-air combustion in inert porous media under the conditions of upstream and downstream combustion wave propagation through the media, Combust. Flame 209 (2019) 74–98.
[20] J.C. Ferguson, S. Sobhani, M. Ihme, Pore-resolved simulations of porous media combustion with conjugate heat transfer, Proc. Combust. Inst. 38 (2021) 2127–2134.
[21] M. Kaviany, Principles of heat transfer in porous media, Mech. Eng. 49 (1991) B103–B104.
[22] J.E.A. Coutinho, M.J.S. de Lemos, Laminar flow with combustion in inert porous media, Int. Commun. Heat Mass Tran. 39 (2012) 896–903.
[23] A.J. Barra, G. Diepvens, J.L. Ellzey, M.R. Henneke, Numerical study of the effects of material properties on flame stabilization in a porous burner, Combust. Flame 134 (2003) 369–379.
[24] J. Shi, M. Mao, H. Li, Y. Liu, Y. Liu, Y. Deng, Influence of chemical kinetics on predictions of performance of syngas production from fuel-rich combustion of CO_2/CH_4 mixture in a two-layer burner, Front. Chem. 7 (2019) 902.
[25] M. Liao, S. Jia, Q. Wang, T.L. Chan, Y. Li, X. Xu, Z. He, Numerical simulation of methane combustion in two-layer porous media under oxy-fuel condition, flow, Turbulence and Combustion 110 (2022) 649–670.
[26] I.F. Macdonald, M.S. El-Sayed, K. Mow, F.A.L. Dullien, Flow through porous media-the Ergun equation revisited, Ind.eng.chem.fundam 18 (1979) 199–208.
[27] E. Achenbach, Heat flow characterstics of packed beds, Exp. Thermal Fluidence 10 (1995) 17–27.
[28] L.B. Youngis, R. Viskanta, Experimental determination of the volumetric heat transfer coefficient between stream of air and ceramic foam, Int. J. Heat Mass Tran. 36 (1993) 1425–1434.
[29] K.V. Dobrego, N.N. Gnesdilov, S.H. Lee, H.K. Choi, Overall chemical kinetics model for partial oxidation of methane in inert porous media, Chem. Eng. J. 144 (2008) 79–87.
[30] P.F. Hsu, J.R. Howell, Measurements of thermal conductivity and optical properties of porous partially stabilized zirconia, Exp. Heat Tran. (1993) 293–313.
[31] A. Stagni, A. Frassoldati, A. Cuoci, T. Faravelli, E. Ranzi, Skeletal mechanism reduction through species-targeted sensitivity analysis, Combust. Flame 163 (2016) 382–393.
[32] A. Cuoci, A. Frassoldati, T. Faravelli, E. Ranzi, OpenSMOKE++: an object-oriented framework for the numerical modeling of reactive systems with detailed kinetic mechanisms, Comput. Phys. Commun. 192 (2015) 237–264.

[33] C. Zheng, L. Cheng, A. Saveliev, Z. Luo, K. Cen, Gas and solid phase temperature measurements of porous media combustion, Proc. Combust. Inst. 33 (2011) 3301–3308.
[34] O. Pickenaecker, K. Pickenaecker, K. Wawrzinek, D. Trimis, F. Jansen, Innovative ceramic materials for porous-medium burners, II, Interceram: Int. Ceram. Rev. 48 (1999) 424–433.
[35] R.V.X. Fu, J.P. Gore, Measurement and correlation of volumetric heat transfer coefficients of cellular ceramics, Exp. Therm. Fluid Sci. 17 (1998) 285–293.